MCAT Institute
Annual Report
94-11

Numerical Simulation of the Flow About the F-18 HARV at High Angle of Attack

Scott M. Murman

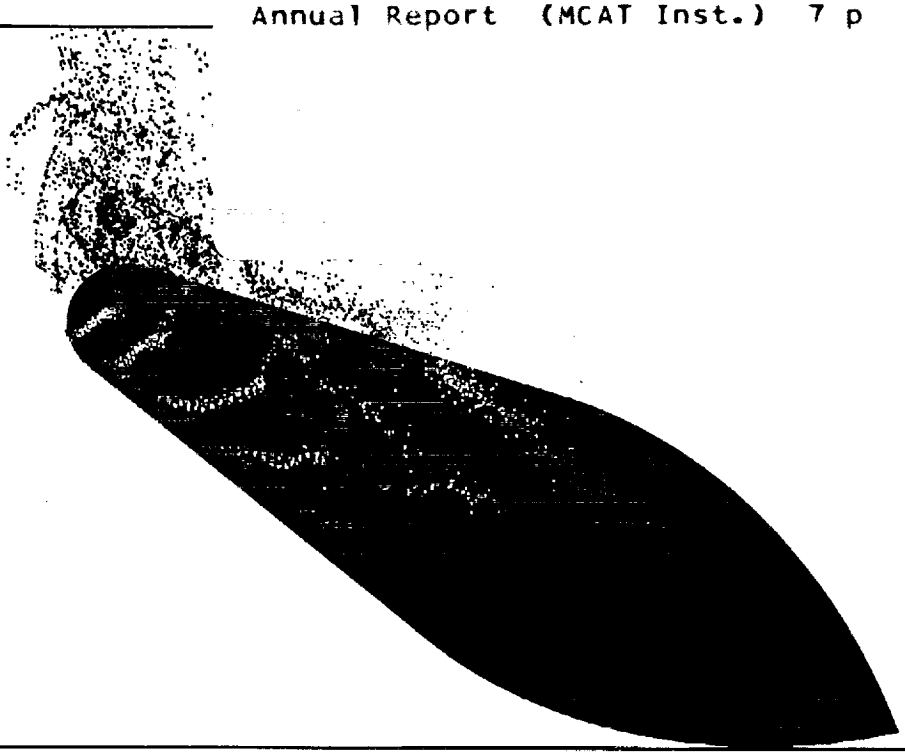

August 1994

NCC2-729

MCAT Institute
3933 Blue Gum Drive
San Jose, CA 95127

Numerical Simulation of the Flow About the F–18 HARV at High Angle of Attack

Annual Report for NASA Grant NCC2–729
August, 1994

Scott M. Murman
Principal Investigator
MCAT Institute, Moffett Field, CA 94035

INTRODUCTION

As part of NASA's High Alpha Technology Program, research has been aimed at developing and extending numerical methods to accurately predict the high Reynolds number flow about the NASA F–18 High Alpha Research Vehicle (HARV) at large angles of attack. The HARV aircraft is equipped with a bi-directional thrust vectoring unit which enables stable, controlled flight through 70° angle of attack. Currently, high-fidelity numerical solutions for the flow about the HARV have been obtained at $\alpha = 30°$, and validated against flight-test data. It is planned to simulate the flow about the HARV through $\alpha = 60°$, and obtain solutions of the same quality as those at the lower angles of attack. This report presents the status of work aimed at extending the HARV computations to the extreme angle of attack range.

The physics of the flow about the HARV changes as the angle of attack is increased from $\alpha = 30°$ to $\alpha = 60°$. At the lower angles of attack, the flowfield is dominated by the formation and subsequent breakdown of the vortices shed from the wing leading-edge extensions (LEX). As the angle of attack increases, the flow about much of the aircraft becomes dominated by an unsteady shedding of the boundary layers, and the convection downstream of these unsteady waves. In order to better understand the physics involved with this unsteady shedding, various computations have been performed using the simpler geometry of a tangent-ogive cylinder at high angle of attack. These computations not only give insight into the physics involved with the full-aircraft geometry, they provide experience and confidence with the numerical code.

RESULTS AND DISCUSSION

A variety of cases have been computed for the ogive-cylinder configuration at high angle of attack. This wide variation in computational studies is possible due to the simplified geometry of the ogive-cylinder (Fig. 1). A single-zone grid with approximately 500,000 grid points can provide a highly accurate simulation of the flowfield, as compared to the multi-zone, several million grid point systems that are required to simulate the complete F–18 HARV aircraft. Two body configurations have been computed: one having a 3.5 caliber tangent-ogive portion with a cylinder portion of 7.0 diameters, and the other having a 3.0 caliber tangent-ogive section with a cylinder region extending 12.0 diameters. The study has thus far focused on comparing two angle of attack and Reynolds number combinations, $\alpha = 40°$ and $60°$, and $Re_D = 80,000$ and $200,000$. Both of these Reynolds numbers are assumed to maintain laminar flow throughout the computational region. This combination of different bodies, Reynolds numbers, and angles of attack provides a wide test-bed for the numerical scheme. This test-bed is further extended by also comparing computational cases having a lateral plane of symmetry with the same cases computed using a periodic grid set-up (Fig. 2). These two computational configurations should provide nearly the same results for computations which are symmetric about the lateral plane of symmetry (this includes all cases computed thus far).

$\alpha = 40°$ Computations

The cases that were computed at $\alpha = 40°$ were generally "well behaved," and displayed many of the general features of unsteady boundary layer shedding. Of importance to note were that the computations with the lateral plane of symmetry and the full periodic grid were identical to the order of round-off error, in terms of both the convergence history, and the final median value of normal force. This same behavior was observed in comparing different numerical algorithms. Figure 3 shows the normal force history for an $\alpha = 40°$, $Re_D = 80,000$ case using the 3.0 caliber ogive cylinder body computed using two distinct algorithms. The F3D algorithm uses flux-vector splitting in the streamwise direction while the Beam and Warming algorithm (B&W) uses a central differencing scheme in the streamwise direction with added numerical dissipation. As can be seen from the force history, both algorithms are showing nearly identical behavior at this angle of attack and Reynolds number.

Two cases were computed using the same ogive-cylinder body at 40° angle of attack, with different Reynolds number, $Re_D = 80,000$ and $200,000$. This shows the difference in shedding frequency and amplitude of the pressure variations as the Reynolds number is increased. Figure 4 shows the computed normal force history for the Reynolds number comparison. It is required to compute to a non-dimensional time of near $\hat{t} = 200$ before the initial transients are removed from the computational domain, and a regular periodic variation in normal force is observed. The normal force oscillates at a frequency of approximately 145 Hz in the $Re_D = 80,000$ computation, and 60 Hz in the $Re_D = 200,000$ computation. The amplitude of the oscillation is increased in the $Re_D = 200,000$ computation. The frequency or the normal force variation and the shedding frequency are the same in the $Re_D = 80,000$ computation, however in the $Re_D = 200,000$ computation the two frequencies are not identical. The shedding frequency at $Re_D = 200,000$ is about 4 times as great as the frequency of the normal force oscillation. The cause of this is not known at this time, and further research is planned to understand the behavior. In order to visualize the shedding of the shear layers from the side of the ogive cylinder, an animation of streaklines released in the unsteady flowfield was created using the UFAT visualization program. A snapshot of this animation is shown is Fig. 5. The shedding waves are clearly visible as the groups of particles, and the convection downstream and rolling into the vortex shed from the nose, can also be seen.

$\alpha = 60°$ Computations

While the cases that were computed at $\alpha = 40°$ were termed well behaved, the computations at $\alpha = 60°$ have thus far been pathologically behaved. However, this is also representative of trends that have been observed in experimental testing, where even small changes in an experimental set-up can lead to large changes in results in the extreme angle of attack range. Where at $\alpha = 40°$ the plane of symmetry and periodic configurations display the same results to the order of round-off error, at $\alpha = 60°$ the two computations show radically dis-similar behavior. Specifically, the lateral force coefficient no longer remains at a nominally zero value in the periodic configuration. This build-up of lateral force influences the other force and moment coefficients to diverge from their "symmetric" values as well. This behavior is not consistent between algorithms, as can be seen by the history of lateral force coefficient shown in Fig. 6. Here, both the F3D and Beam and Warming algorithms

show a build-up in lateral force, but the mean values and amplitudes of motion are different. In fact, the side forces seen in the two computations are of opposite sign. This behavior has been extensively investigated in order to better understand how a nominally symmetric algorithm can generate asymmetric solutions. Progress has been made, however any results which could be stated now would be conjecture.

F–18 Grid Generation

An ongoing effort has been underway to generate a new grid system for the F–18 HARV aircraft. This is motivated by several factors, most important being the computational requirements of simulating the unsteady shedding at the extreme angles of attack. As has been seen with the ogive-cylinder computations, the computational time required to remove the initial transients from the solution is very significant. In order to make this feasible for a full-aircraft grid system, the grid points must be used in the most efficient manner possible. This must be done while improving the overall grid resolution of the system to provide accurate convection of the shedding waves downstream. To achieve these goals a grid system based on "background" cartesian meshes with embedded "viscous wall" meshes is being developed. An overview of this method as applied to the F–18 HARV forebody and LEX region is shown in Fig. 7. Separate grids are generated for the forebody and LEX regions and then embedded in the background, inviscid cartesian grid. Work is underway to model the entire aircraft in this manner.

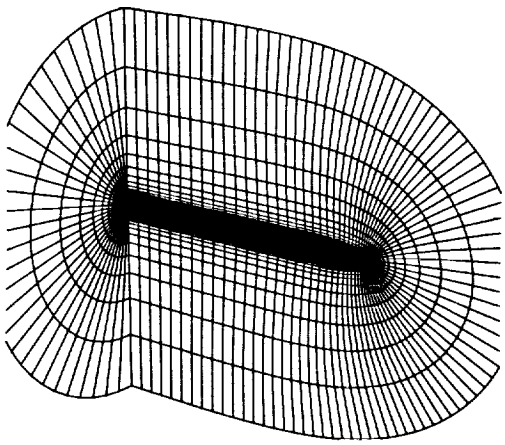

Fig. 1. Tangent-ogive cylinder grid configuration.

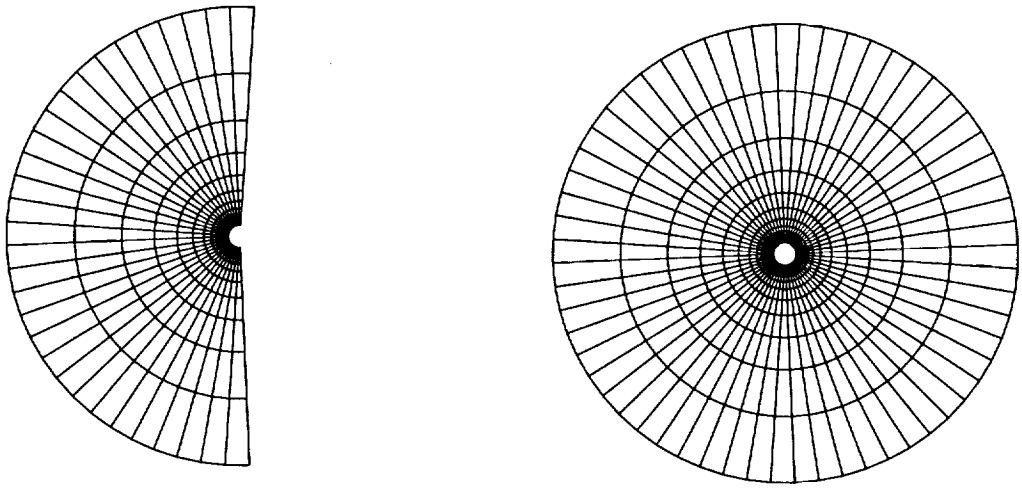

a. Lateral plane of symmetry.

b. Periodic grid.

Fig. 2. Symmetric grid boundary conditions.

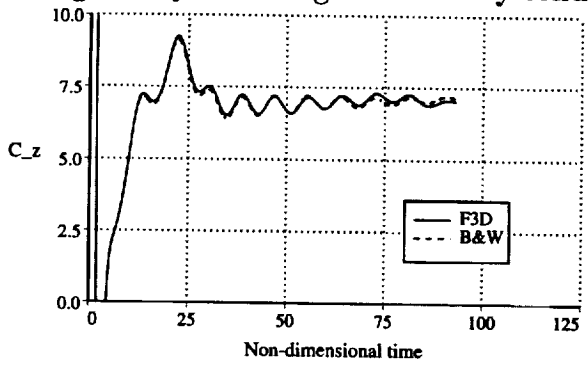

Fig. 3. Normal force history at $\alpha = 40°$, $Re_D = 80,000$.

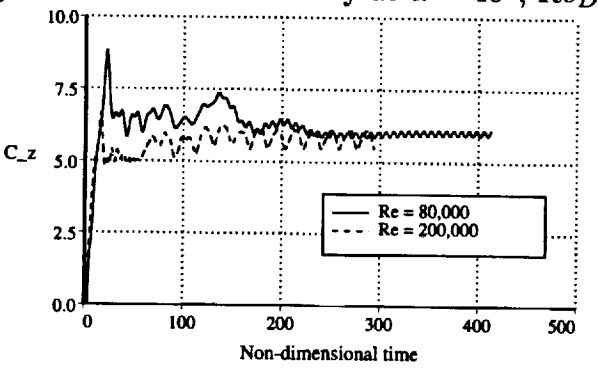

Fig. 4. Normal force history at $\alpha = 40°$.

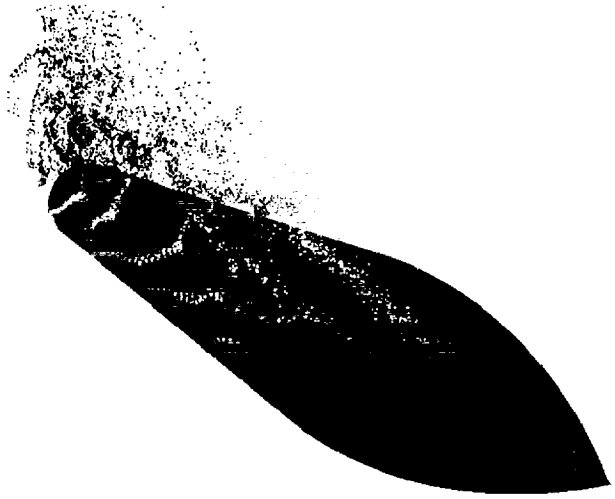

Fig. 5. Shear-layer shedding at $\alpha = 40°$, $Re_D = 200,000$.

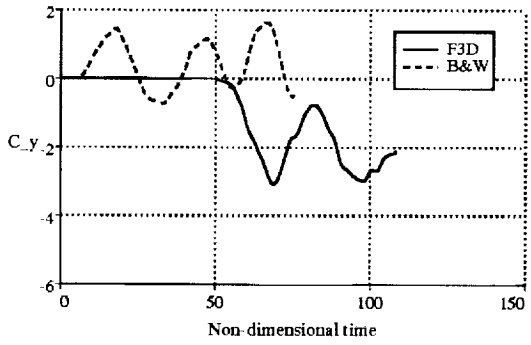

Fig. 6. Lateral force history at $\alpha = 60°$, $Re_D = 200,000$.

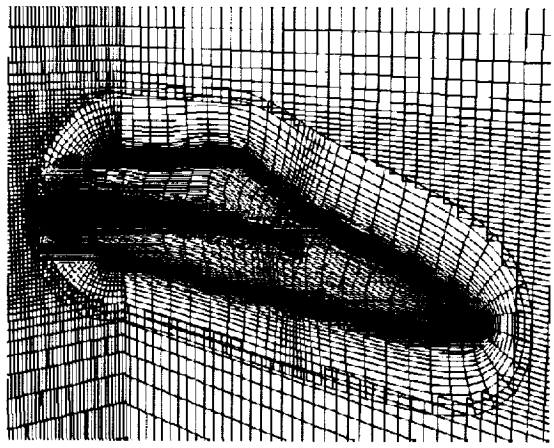

Fig. 7. F–18 forebody/LEX grid system.